JOURNAL OF MICROENCAPSULATION
2021, VOL. 38, NO. 6, 365–380
https://doi.org/10.1080/02652048.2021.1948622

Taylor & Francis
Taylor & Francis Group

ORIGINAL ARTICLE

Microparticles loaded with fish oil: stability studies, food application and sensory evaluation

Ana Lúcia Fadini[a,e], Izabela Dutra Alvim[a], Camila Augusto Carazzato[b], Katyri Bezerra de Freitas Paganotti[b], Ana Maria Rauen de Oliveira Miguel[c] and Rodney Alexandre Ferreira Rodrigues[d,e]

[a]Cereal Chocotec, Institute of Food Technology, Campinas, Brazil; [b]School of Food Science, University of São Paulo, ESALQ, Piracicaba, Brazil; [c]CCQA, Institute of Food Technology, Campinas, Brazil; [d]Phytochemistry Division, CPQBA, University of Campinas, Paulínia, Brazil; [e]Department of Food and Nutrition, School of Food Engineering, University of Campinas, Campinas, Brazil

ABSTRACT

Aim: Evaluate the stability of microparticles loaded with fish oil produced by spray drying, spray chilling and by the combination of these techniques (double-shell) and use the microparticles for food application.

Methods: Samples were stored for 180 days at 6 °C and 24 °C (75% RH). Performed investigations included encapsulation efficiency, moisture content, a_w, size (laser scattering), colour (L*, a*, b*), polyunsaturated fatty acids (PUFAs) (GC), thermal behaviour (DSC) and crystalline structure (XRD).

Results: Double-shell microparticles containing 26 wt% core material, 22.74 ± 0.02 μm ($D_{0.5}$) and 2.05 ± 0.03 span index, 1.262 ± 0.026 wt% moisture content and 0.240 ± 0.001 of a_w had PUFAs retention higher than 90 wt% during storage at 6 °C without changes in crystalline structure (β′-type crystals) and melting temperature (54 °C). The sensory evaluation suggested low fish oil release in oral phase digestion.

Conclusions: Double-shell microparticles were effective to protect and deliver PUFAs.

ARTICLE HISTORY
Received 20 January 2021
Accepted 23 June 2021

KEYWORDS
Microencapsulation; double-shell; EPA; DHA; storage; sensory acceptance

1. Introduction

Eicosapentaenoic acid (EPA; 20:5n-3) and docosahexaenoic acid (DHA; 22:6n-3), found in high amounts in fatty fish, appear to be functionally the most important omega-3 fatty acids (Calder 2014). An adequate intake of omega-3 polyunsaturated fatty acids (PUFAs) is required for human growth and development (Al-Ghannami *et al.* 2019) because endogenous synthesis of EPA in humans is very limited and depends on the intake of alfa-linolenic acid (ALA; 18:3n3); additionally, DHA production is the result of additional elongation and desaturation of EPA (Murff and Edwards 2014).

Many health benefits are attributed to omega-3 fatty acids, such as anti-inflammatory properties, prevention of cardiovascular disease, effects against some types of cancer and autoimmune disorders and the normal functional development of the brain and retina (Ghorbanzade *et al.* 2017, Zárate *et al.* 2017, Di Giorgio *et al.* 2019, Haimeur *et al.* 2019).

The food industry plays an important role in the supply of enriched foods with EPA and DHA, but the direct incorporation of fish oil into foods is restricted due to secondary and tertiary lipid oxidation compounds that result in an undesirable flavour in addition to nutritional losses (Serfert *et al.* 2010, Aghbashlo *et al.* 2013, Binsi *et al.* 2017, Yeşilsu and Özyurt 2019).

Encapsulation is an alternative for protecting unsaturated fatty acids against oxidation and reactions caused by factors such as light, temperature, oxygen and humidity, and can increase the shelf life, mask unpleasant flavours and allow the delivery of fish oil. Spray drying microencapsulation is considered the least expensive and most appropriate technique for this purpose (Encina *et al.* 2016, Binsi *et al.* 2017, Chatterjee and Judeh 2017, Di Giorgio *et al.* 2019).

The spray-drying process uses water-soluble wall materials based on carbohydrates or proteins that are not suitable for controlled-release applications, and this characteristic could lead to oil flavour perception in the oral phase of digestion (Cho *et al.* 2003, Fadini *et al.* 2019). To overcome this limitation, Fadini *et al.* (2018) studied an innovative strategy in which fish oil was first microencapsulated by spray drying and then by spray chilling, techniques that can be easily used

CONTACT Ana Lúcia Fadini fadini@ital.sp.gov.br Cereal Chocotec, Institute of Food Technology, Campinas 13070-178, Brazil
This article has been republished with minor changes. These changes do not impact the academic content of the article.

for industrial-scale microparticle production and Fadini *et al.* (2019) conducted a second study to optimise the composition of the lipid matrix and core concentration of these double-shell microparticles. Therefore, the aim of the current study was to evaluate the stability of microparticles loaded with fish oil produced by spray drying, spray chilling and by the combination of these two techniques (double-shell microparticles), during 180 days of storage at different temperatures in order to confirm if the double encapsulation could increase the fish oil PUFAs protection and also delay the fish oil flavour perception. The feasibility of using the studied microparticles for food enrichment with EPA and DHA was evaluated using a sensory acceptance test with one hundred and twenty consumers. This study approach since the microparticles production, the evaluation of their stability during storage and performance during the food application until the sensory evaluation is very rare in the literature.

2. Experimental

2.1. Materials

Fish oil W3-MEG-3 4020 EE Oil® (DSM, Canada) and fish oil Incromega E3322-LQ-(LK) (Croda Europe Limited, England) were used as core material. In the formation of spray-dried microparticles acacia gum Encapsia® (Nexira, France) and skimmed milk powder (Nestlé, Brazil) were used as emulsifiers and wall materials, grape juice (Aurora, Brazil) to mask unpleasant flavours and polysorbate 80 Tween® 80 (Synth, Brazil) as emulsifier. In the formation of spray-chilled microparticles a lipid matrix composed by the combination of two lipid carriers zero trans was used, a 100% hydrogenated palm oil (A. Azevedo Óleos Vegetais, Brazil) (PF) whose fatty acid composition was 0.42% 12:0; 0.88% 14:0; 38.19% 16:0; 0.12% 17:0; 55.19% 18:0; 0.14% 18:1; 0.51% 20:0; 0.07% 22:0; 0.08% 24:0 and the vegetable fat AL Lette K39LT® (Cargill, Brazil) (VF) whose fatty acid composition was 0.14% 6:0; 2.65% 8:0; 2.71% 10:0; 40.29% 12:0; 13.67% 14:0; 10.26% 16:0; 24.44% 18:0; 0.49% 18:1; 0.72% 18:2; 0.24% 20:0. These lipid carriers were selected because they are common food ingredients and have a thermal resistance that could ensure the handling of the microparticles. Polyglycerol polyricinoleate PGPR 4150® (Palsgaard, Denmark) was used as emulsifier. Chocolate dragees were produced with a milk and dark chocolate blend (Harald, Brazil) and extruded cereals (Nestlé, Brazil). The cereal bar ingredients were purchased in a local market (cereals, glucose syrup, inverted sugar, honey, dried fruits, such as blueberries, cranberries and raisins, Brazilian nuts and other ingredients currently used in this product). The Supelco 37 FAME Mix standard (Sigma-Aldrich, USA) was used in the gas chromatography analysis. Chemical reagents were purchased from Merck (Germany).

2.2. Methods

2.2.1. Microparticle production

The spray-dried microparticles wall material was composed by a mixture of acacia gum, skimmed milk powder and grape juice at a ratio of 2.6:1.8:1.0 (d.b.). The emulsion total solid content was 30 wt% and the fish oil content was 20% in the solid. The wall materials were previously dissolved in distilled water and the fish oil and the Tween® 80 (0.48 g/100 g total emulsion) were added to the continuous phase. The emulsion was obtained using an Ultra Turrax® (T18, IKA, Germany) (15,000 rpm for 3 min.). Spray-dried microparticles were produced using a mini spray dryer (B-290, Büchi, Switzerland). The inlet and outlet temperatures were 150 ± 1 °C and 76 ± 3 °C, respectively. The spray nozzle (0.7 mm) was maintained at 21 °C. The feed sample rate was 10 ml/min and the drying air flow rate was 10,017 ml/min. The spray-dried microparticles loaded with fish oil were named SD-M.

Spray-chilled microparticles were produced in the mini spray-dryer connected to a dehumidifier (B-296, Büchi, Flawil, Switzerland). The inlet temperature was 7 ± 3 °C, and the spray nozzle (2.0 mm) was maintained at 80 °C. The feed sample rate was approximately 10 ml/min and the air flow rate was 12,366 ml/min. Two different types of microparticles were produced by spray chilling. For the first type of spray-chilled microparticles, the fish oil was added to the molten lipid wall material (80 °C) composed by PF and VF and the mixture was sprayed into the cold chamber. This spray-chilled microparticles sample loaded with fish oil was named SCFO. For the second type of spray-chilled microparticles, three different concentrations of spray-dried microparticles loaded with fish oil (SD-M) (26 wt%, 40 wt% and 50 wt%) were used as core material in order to produce the double-shell microparticles. The double-shell microparticles sample loaded with 26 wt% of SD-M was named DS26, the double-shell microparticles sample loaded with 40 wt% of SD-M was named DS40 and the sample loaded with 50 wt% of SD-M was named DS50. The SD-M were dispersed in the molten lipid carriers (80 °C) composed by PF and VF, PGPR was added at a concentration of 4.8 wt% and the dispersions were sprayed into the cold chamber. The double-shell

Table 1. Solid lipid microparticle compositions, including a control sample without core material, a spray-chilled microparticle loaded with fish oil and the double-shell microparticles samples with three different core material concentrations.

Samples	PF/VF ratio (lipid matrix)	Core Material (wt%)
PF/VF 1:1 (control sample)	1:1	–
SCFO (spray chilled microparticle loaded with fish oil)	1:1	5.5 (FO)
DS26 (double-shell microparticle / 26 wt% core material)	1:1	26 (SD-M)
DS40 (double-shell microparticle / 40 wt% core material)	1:1.8	40 (SD-M)
DS50 (double-shell microparticle / 50 wt% core material)	1:1.5	50 (SD-M)

FO: fish oil; SD-M: spray-dried microparticles loaded with fish oil; PF: 100% hydrogenated palm oil; VF: vegetable fat obtained from fully hydrogenated and interesterified vegetable oils; SCFO: spray-chilled microparticles loaded with fish oil; DS26: double-shell microparticles loaded with 26 wt% of SD-M; DS40: double-shell microparticles loaded with 40 %wt of SD-M; DS50: double-shell microparticles loaded with 50 %wt of SD-M.

microparticles compositions were selected from the results obtained in a previous work (Fadini *et al*. 2019). All studied samples are presented in Table 1, excepted the spray-dried microparticles composition that is described above.

2.2.2. Encapsulation efficiency (EE) of spray-dried microparticle (SD-M)

SD-M surface oil (SO) was measured as described by Bae and Lee (2008) with some modifications. 15 ml of hexane was added to 1.5 g of microparticles, the mixture was stirred in a glass jar with a lid for 2 min, filtered through a Whatman filter paper No 1, and the remaining powder was rinsed three times with 20 ml of hexane. The filtrated solution was evaporated at 70 °C, and the SO calculated. The SD-M total oil (TO) was extracted by adding chloroform/methanol/water in the proportions of 1:2:0.8 and 2:2:1.8, respectively, to 2.5 g of microparticles. The chloroform phase containing the extracted oil was separated and evaporated at 100 °C, and the TO was calculated (Bligh and Dyer 1959). The EE was calculated according to Ramos *et al*. (2021).

2.2.3. Characterisation of microencapsulated fish oil powder during storage

This study was conducted during 180 days in order to better understand the main factors affecting the microparticles shelf-life. Samples were stored at 6 ± 2 °C and 24 ± 1 °C in open pots placed inside desiccators at 75% RH, since this relative humidity can represent the conditions to which these microparticles would be exposed when used to enrich food products with high water activities.

2.2.3.1. Moisture content and water activity (a_w).

The moisture content was gravimetrically determined as described by Lavanya *et al*. (2020), with some adjustments. Approximately 1.5 g of microparticles were placed in an aluminium pan and dried in an oven at 105 °C for 20 h. The a_w was measured with a water activity metre (4TEV AquaLab, Decagon Devices Inc., Pullman, USA) at 25.0 ± 0.5 °C. The analyses were performed in triplicate at 0, 90 and 180 days of storage.

2.2.3.2. Particle size and size distribution.

A laser particle size analyser LA-950V2 (Horiba, Kyoto, Japan) was used to determine the mean diameter ($D_{4,3}$) and microparticle size distribution by using the characteristic parameters $D_{0.1}$, $D_{0.5}$ and $D_{0.9}$, which represent the diameters of 10%, 50% and 90% accumulated distribution of the total particles, respectively. SD-M sample was dispersed in absolute ethanol and solid lipid microparticles (SLMs) in a solution of polyoxyethylene (20) sorbitan monolaurate (0.5 g/100 g, Tween 20) (Alvim *et al*. 2016). The span index was calculated according to Fadini *et al*. (2019). The measurements ($n = 6$) were made at days 0 and 180.

2.2.3.3. Colour.

Was evaluated with a Chroma metre (Konica Minolta, CR-410, Tokyo, Japan) using the L^*, a^*, and b^* indexes. The results are expressed as the average of 10 measurements made at 0, 90 and 180 days of storage. The L* value represents the lightness-darkness dimension; a* the red-green dimension; and b* the yellow-blue dimension. The overall colour difference (ΔE^*) was calculated according to Lacerda *et al*. (2016).

2.2.3.4. Morphology.

After 180 days of storage the samples SCFO, DS26, DS40 and DS50 were visualised in a scanning electron microscope (DSM 940 A FOCUS, Zeiss, Germany) equipped with a digital camera (SMZ 745 T, Nikon, Japan) (200× magnification). Microparticles were covered with a gold layer, and an accelerating voltage of 5 kV was used.

2.2.3.5. EPA and DHA content.

EPA and DHA losses after spray-chilled microparticle production were used

to calculate the process encapsulation efficiency by comparing the microparticle PUFAs concentration with the initial (theoretical) concentration of these PUFAs in the feeding material. On the other hand, the losses reported during storage are the difference in EPA and DHA content between stored and newly produced samples. The PUFAs content of the free fish oil was evaluated during the 180 days of storage as a control.

The total oil of the SD-M sample and double-shell samples were extracted as described at the item 2.2.2. The SCFO sample was totally composed by lipids, therefore no oil extraction prior to chromatographic analysis was necessary.

The dried lipid extract was esterified with a solution of ammonium chloride and sulphuric acid in methanol (Hartman and Lago 1973), and the fatty acid composition was determined by separation on a fused silica capillary column 100 m in length with a 0.25 mm inner diameter and a 0.20 μm film thickness (CP-Sil 88, Agilent) using an Agilent 7890 A gas chromatograph equipped with a split injector and a flame ionisation detector. The fatty acids were identified by comparing the retention times to those of the standards (Supelco 37 Component FAME Mix) (AOCS 2017) and were quantified by area normalisation. The results were expressed in g/100 g of sample (Food Standards Agency 2002). The analysis was performed in triplicate at 0, 90 and 180 days of storage.

The best performing double-shell microparticle sample, the SCFO and a control sample (empty microparticles) were evaluated to determine their thermal properties and polymorphic crystal forms during a second storage stability study. The microparticles samples were stored at 25 ± 1 °C in closed containers and evaluated at 0, 7, 14, 21, 28, 60, 90 and 120 days of storage. The used methodologies are described below.

2.2.3.6. Thermal behaviour by differential scanning calorimetry (DSC). Thermal evaluation was performed by differential scanning calorimetry (DSC; TA Thermal Analyser, Q2000 V4.7A, coupled to a RCS90 refrigerated cooling system, TA Instruments, Waters LLC, USA). Considering that possible interaction between the core material (fish oil or SD-M) and the lipid matrix could result in variations in the enthalpy curve, a control sample (empty microparticles) was included in the study. The evaluated samples were fish oil, vegetable fat (VF), 100% hydrogenated palm oil (PF), a mixture of PF and VF 1:1 (control sample, empty microparticles), spray-chilled microparticles loaded with fish oil (SCFO) and the double-shell microparticles (DS26) loaded with 26 wt% of spray-dried microparticles loaded with fish oil (SD-M). For the fish oil analysis, samples of 8–9 mg were placed in hermetically sealed aluminium pans. The operation conditions were as follows: the samples were heated to 80 °C and maintained for 10 min, cooled to −40 °C (10 °C/min) for 30 min and then heated to 80 °C at 5 °C/min, method Cj 1–94 (AOCS 2017) to obtain the crystallisation and fusion curves. For the individual lipid carriers (VF and PF), the control sample, the SCFO and the DS26 sample (7–8 mg), the operation conditions were adapted from Lopes *et al.* (2015) and the samples were stabilised at 15 °C for 10 min and then heated to 100 °C (5 °C/min) to obtain the fusion curve. The analysis was performed in triplicate and an empty pan was used as a reference.

2.2.3.7. Crystalline structure. A Philips X-ray diffractometer (Analytical, X Ray X'Pert-MPD, Netherlands) using the Bragg-Brentano (θ:2θ) geometry with X-rays of $\lambda = 1.54056$ Å originating from a Cu Kα source with a voltage of 40 kV and a current of 40 mA was used to determine the fat crystalline structure of the individual lipid carriers (VF and PF), a control sample (empty microparticles), SCFO and DS26 samples. The diffraction was measured in the 2θ range from 5° to 40°, at a rate of 0.02°/s. The polymorphic forms were identified from the characteristic short spacings of each fat crystal (Oriani *et al.* 2018). According to Marangoni (2005), the main application of powder X-ray diffraction is qualitative analysis.

2.2.4. Food application and sensory acceptance test

During food application the solid lipid microparticles should not be exposed to temperatures higher than the melting peak temperature of their lipid matrix and the food product characteristics at that point must guarantee a proper homogenisation of the added microparticles powder. Therefore, one of the selected products was based on lipids (chocolate dragees) and the microparticles were incorporated in the molten chocolate at 45 °C, previously to the panning process and the other product was based on sugars (cereal bars) and the microparticles were incorporated in the product lamination step, at 38–40 °C.

The chocolate dragees were produced in a rotating pan (JAA110E, Incal, Brazil) and the cereal bars in a pilot plant (Braslaer, Brazil). These products were enriched with 40 mg of the sum of EPA and DHA per serving portion (25 and 30 g of dragees and cereal bar, respectively) through the addition of those microparticles that had the highest EPA and DHA retention during storage. One hundred and twenty untrained

consumers of these products, of both genders and more than 18 years old, evaluated the samples to determine the linking colour, aroma, taste, texture and overall impression using a 9-point structured hedonic scale with the end anchors 'extremely dislike' and 'extremely like' (Stone and Sidel 2004). The consumers previously received information about the health benefits of PUFAs and were informed that the products were enriched with omega-3 EPA and DHA. This research was approved by the Research Ethics Committee of the Max Planck Faculty in Brazil (CAAE 59078216.5.0000.8053).

2.2.5. Statistical analysis

The results were evaluated by analysis of variance (ANOVA) followed by a Tukey test (95% confidence interval) using the Statistica® 12 (StatSoft Inc., USA) program to compare the differences between the mean values.

3. Results and discussion

3.1. Encapsulation efficiency (EE) of spray-dried microparticle (SD-M)

In general the EE may be affected by many factors as emulsion composition, pH, type and content of emulsifiers, droplet size, type of wall material, fish oil concentration, and spray drying parameters as inlet and outlet air temperature, air flow rate, humidity and type of atomisation (Encina *et al.* 2016; Mohammed *et al.* 2020).

The EE of the SD-M was 94.64 ± 0.17%, indicating a high content of fish oil entrapped inside the microparticles that could be attributed to the use of wall materials with emulsifing properties, to the emulsion characteristics and also to the process conditions used, as inlet temperature, feed sample rate and gas flow. The oil-droplets in the powders, observed through optical microscopy images (data not shown), were smaller than the particle size. Large oil droplets and small particles could result in more non-encapsulated oil (Linke *et al.* 2020b). Geranpour *et al.* (2020) pointed out that a lower amount of non-encapsulated oil could be found in larger particles due to the lower proportion of the surface and volume, but also could be found in smaller particles because of the higher drying rate in the begging of the drying process. The amount of superficial oil can be affected by the water migration rate during the drying process, the crust formation and microparticles morphology, in other words, the driven force of heat and mass transfer will impact the microparticles characteristics (Ramos *et al.* 2021).

Similar results of EE were reported in the literature for spray-dried microparticles loaded with fish oil using different ratios of maltodextrin DE 21 and soy protein isolate as wall materials, inlet and outlet temperatures of 160 °C and 85 °C, respectively, with EE ranging from 53.82% to 93.56% as a consequence of different protein to oil ratios and different homogenisation pressure used in the emulsion preparation (Linke *et al.* 2020c). EE between 90.08% and 92.51% and non-encapsulated oil ranging from 2.27% to 2.91% were obtained for spray-dried microparticles loaded with fish oil produced with soy protein isolate and maltodextrin DE 21 as wall materials (2% and 29% w/w of emulsion, respectively). The emulsions were prepared under inert and atmospheric conditions and nitrogen or air were used as drying mediums. The authors suggested that the difference in the results could be related to the size of oil droplets and powder particles (Linke *et al.* 2020b). Hinnenkamp *et al.* (2021) microencapsulated fish oil by spray drying using as wall materials intact and hydrolysed whey protein concentrate, maltodextrin 15 DE and a blend of phospholipid-rich whey coproduct and obtained microparticle powders with EE ranging from 92.6% to 96.8% and attributed these high values to the high ratio of maltodextrin to protein used in the wall material since the drying parameters were constant.

Although the high EE obtained at the present study, the SD-M have water-soluble wall materials, therefore this sample was used as core material for producing double-shell microparticles, in order to increase the oxidative protection and delay the fish oil delivery in food application.

3.2. Characterisation of microencapsulated fish oil powder during storage

3.2.1. Moisture content and water activity (a_w)

The moisture content of the newly produced microparticles were 2.870 ± 0.057 wt% (SD-M), 0.990 ± 0.010 wt% (SCFO), 1.262 ± 0.026 wt% (DS26), 1.720 ± 0.030 wt% (DS40) and 2.200 ± 0.032 wt% (DS50) (Table 2).

The storage time influenced the moisture gain, which continuously increased, mainly between zero and 90 days. Between 90 and 180 days, the DS26 sample did not show any variation in this parameter at 24 ± 1 °C and the SCFO showed no variation at either storage temperature (Table 2, lowercase letters).

Table 2. Moisture content and water activity of spray-dried microparticles loaded with fish oil (SD-M), spray-chilled microparticles loaded with fish oil (SCFO), double-shell microparticles loaded with 26 wt% of SD-M (DS26), double-shell microparticles loaded with 40 wt% of SD-M (DS40) and double-shell microparticles loaded with 50 wt% of SD-M (DS50) at zero, 90 and 180 days of storage at 6 ± 2 °C and 24 ± 1 °C (mean ± SD, where $n = 3$).

	Storage at 6 ± 2 °C		Storage at 24 ± 1 °C	
Days	Moisture content (wt%)	Water activity (a_w)	Moisture content (wt%)	Water activity (a_w)
	SD-M Sample - spray-dried microparticles loaded with fish oil			
0	$2.870 \pm 0.057^{c,A}$	$0.178 \pm 0.006^{c,A}$	$2.870 \pm 0.057^{c,A}$	$0.178 \pm 0.006^{c,A}$
90	$14.637 \pm 0.064^{b,B}$	$0.669 \pm 0.002^{b,B}$	$16.138 \pm 0.174^{b,A}$	$0.698 \pm 0.001^{b,A}$
180	$17.797 \pm 0.246^{a,A}$	$0.711 \pm 0.001^{a,A}$	$16.575 \pm 0.112^{a,B}$	$0.709 \pm 0.002^{a,A}$
	SCFO Sample - spray-chilled microparticles loaded with fish oil			
0	$0.990 \pm 0.010^{a,A}$	$0.433 \pm 0.004^{b,A}$	$0.990 \pm 0.010^{b,A}$	$0.433 \pm 0.004^{b,A}$
90	$1.205 \pm 0.113^{a,A}$	$0.439 \pm 0.008^{b,A}$	$1.475 \pm 0.189^{a,A}$	$0.440 \pm 0.003^{b,A}$
180	$1.082 \pm 0.202^{a,B}$	$0.467 \pm 0.006^{a,A}$	$1.719 \pm 0.121^{a,A}$	$0.467 \pm 0.001^{a,A}$
	DS26 Sample - double-shell microparticles loaded with 26 wt% of SD-M			
0	$1.262 \pm 0.026^{c,A}$	$0.240 \pm 0.001^{c,A}$	$1.262 \pm 0.026^{b,A}$	$0.240 \pm 0.001^{c,A}$
90	$4.866 \pm 0.062^{b,B}$	$0.697 \pm 0.003^{a,B}$	$5.276 \pm 0.107^{a,A}$	$0.710 \pm 0.001^{b,A}$
180	$5.643 \pm 0.101^{a,A}$	$0.659 \pm 0.002^{b,B}$	$5.330 \pm 0.081^{a,B}$	$0.721 \pm 0.001^{a,A}$
	DS40 Sample - double-shell microparticles loaded with 40 wt% of SD-M			
0	$1.720 \pm 0.030^{c,A}$	$0.200 \pm 0.004^{c,A}$	$1.720 \pm 0.030^{c,A}$	$0.290 \pm 0.004^{c,A}$
90	$7.303 \pm 0.015^{b,B}$	$0.694 \pm 0.003^{a,B}$	$7.596 \pm 0.041^{b,A}$	$0.720 \pm 0.001^{b,A}$
180	$7.901 \pm 0.166^{a,A}$	$0.668 \pm 0.002^{b,B}$	$7.829 \pm 0.064^{a,A}$	$0.728 \pm 0.002^{a,A}$
	DS50 Sample - double-shell microparticles loaded with 50 wt% of SD-M			
0	$2.200 \pm 0.032^{c,A}$	$0.217 \pm 0.005^{c,A}$	$2.200 \pm 0.032^{c,A}$	$0.217 \pm 0.005^{c,A}$
90	$8.496 \pm 0.066^{b,B}$	$0.698 \pm 0.001^{b,B}$	$9.132 \pm 0.057^{b,A}$	$0.709 \pm 0.001^{b,A}$
180	$10.358 \pm 0.340^{a,A}$	$0.714 \pm 0.003^{a,B}$	$9.471 \pm 0.064^{a,B}$	$0.732 \pm 0.000^{a,A}$

Different lowercase letters for the same sample at different storage times but the same temperature show significant differences among values ($p < 0.05$). Different uppercase letters for the same sample at the same storage time but different temperatures show significant differences among values ($p < 0.05$).

Temperature also influenced the moisture gain, but less than storage time. At both storage temperatures, double-shell microparticles samples DS40 and DS50 gained more moisture which could have been caused by the characteristics of the core material (SD-M), that possibly made the lipid matrix less compact, or some core material may have remained near or at the microparticle surface. As expected, SCFO showed the lowest moisture content during storage at both temperatures (Table 2, uppercase letters).

In general, the SD-M sample exhibited a higher moisture gain, which can be attributed to its hydrophilic wall material and small particle size; additionally, this sample showed a physical change (caking) during the first month of storage. High moisture content can cause physical, textural, chemical, and microbiological changes in the microparticles (Lavanya *et al.* 2020).

Water activity is an important parameter for powdered product quality (Bakry *et al.* 2016), and the lipid oxidation rate may increase at a a_w below 0.2 (Labuza *et al.* 2006) and decrease at a_w above 0.7 due to the dilution of oxidation catalysts (Croguennec 2016).

The a_w values continuously increased up to 180 days, except for the DS26 and DS40 samples stored at 6 ± 2 °C. The SCFO did not show differences in this parameter between zero and 90 days of storage, but a_w slightly increased between 90 and 180 days at both temperatures (Table 2, lowercase letters).

Samples stored at 24 ± 1 °C showed higher a_w than those stored at 6 ± 2 °C (Table 2, uppercase letters). According to Labuza *et al.* (2006), the a_w of dehydrated foods can change if the package used is moisture permeable and when impermeable packages are subject to an upward temperature shift. Different temperatures can affect the a_w since the water binding, dissociation of water, and solubility of solutes in water, among other factors, will be changed (Roudaut and Debeaufort 2010).

At 180 days of storage, the SCFO presented the lowest a_w, confirming that the changes observed in double-shell microparticles could be attributed to the hydrophilic core material. During storage, samples were placed in open containers inside desiccators at 75% RH to accelerate degradation reactions; however, the use of a water vapour barrier package during storage and commercialisation of double-shell microparticles is recommended. The differences in lipid wall material composition showed no influence on moisture content and a_w values.

Similar moisture content and a_w results are reported in the literature. Lavanya *et al.* (2020) obtained spray-dried microparticles loaded with fish oil with moisture content from 2.19 to 3.20% (db) and a_w values from 0.35 to 0.48, which are considered good to have a safe product during the shelf life and for the high quality standards of dried powders in the

Table 3. Particle size of spray-chilled microparticles loaded with fish oil (SCFO), double-shell microparticles loaded with 26 wt% of SD-M (DS26), double-shell microparticles loaded with 40 wt% of SD-M (DS40) and double-shell microparticles loaded with 50 wt% of SD-M (DS50) at zero and 180 days of storage at 6 ± 2 °C and 24 ± 1 °C (mean ± SD, where $n = 6$).

	Storage at 6 ± 2 °C			Storage at 24 ± 1 °C		
Storage time (days)	$D_{4,3}$ (μm)	$D_{0.5}$ (μm)	Span index	$D_{4,3}$ (μm)	$D_{0.5}$ (μm)	Span index
	SCFO Sample - spray-chilled microparticles loaded with fish oil					
0	$18.57 \pm 0.18^{b,A}$	$17.65 \pm 0.13^{b,A}$	$1.71 \pm 0.01^{a,A}$	$18.57 \pm 0.18^{b,A}$	$17.65 \pm 0.13^{b,A}$	$1.71 \pm 0.01^{a,A}$
180	$25.23 \pm 0.15^{a,B}$	$25.76 \pm 0.11^{a,B}$	$1.40 \pm 0.01^{b,A}$	$34.43 \pm 0.24^{a,A}$	$33.33 \pm 0.18^{a,A}$	$1.38 \pm 0.01^{b,B}$
	DS26 Sample - double-shell microparticles loaded with 26 wt% of SD-M					
0	$30.69 \pm 0.33^{b,A}$	$22.74 \pm 0.02^{b,A}$	$2.05 \pm 0.03^{a,A}$	$30.69 \pm 0.33^{b,A}$	$22.74 \pm 0.02^{b,A}$	$2.05 \pm 0.03^{a,A}$
180	$54.76 \pm 0.16^{a,B}$	$49.79 \pm 0.57^{a,B}$	$1.37 \pm 0.02^{b,B}$	$60.45 \pm 1.32^{a,A}$	$51.60 \pm 0.57^{a,A}$	$1.77 \pm 0.10^{b,A}$
	DS40 Sample - double-shell microparticles loaded with 40 wt% of SD-M					
0	$47.08 \pm 0.43^{b,A}$	$29.38 \pm 0.01^{b,A}$	$4.26 \pm 0.10^{a,A}$	$47.08 \pm 0.43^{b,A}$	$29.38 \pm 0.01^{b,A}$	$4.26 \pm 0.10^{a,A}$
180	$56.77 \pm 0.81^{a,B}$	$52.46 \pm 0.24^{a,B}$	$1.29 \pm 0.04^{b,B}$	$76.05 \pm 1.15^{a,A}$	$70.35 \pm 0.49^{a,A}$	$1.85 \pm 0.03^{b,A}$
	DS50 Sample - double-shell microparticles loaded with 50 wt% of SD-M					
0	$71.79 \pm 0.41^{b,A}$	$52.60 \pm 0.07^{b,A}$	$3.17 \pm 0.04^{a,A}$	$71.79 \pm 0.41^{b,A}$	$52.60 \pm 0.07^{b,A}$	$3.17 \pm 0.04^{a,A}$
180	$78.42 \pm 1.15^{a,B}$	$55.25 \pm 0.28^{a,B}$	$3.25 \pm 0.08^{a,A}$	$83.97 \pm 0.83^{a,A}$	$72.11 \pm 0.40^{a,A}$	$2.04 \pm 0.03^{b,B}$

SD-M: spray-dried microparticles loaded with fish oil.
Different lowercase letters for the same sample at different storage times but the same temperature show significant differences among values ($p < 0.05$). Different uppercase letters for the same sample at the same storage time but different temperatures show significant differences among values ($p < 0.05$).

food industry. Salvim *et al.* (2015) produced SLMs from a suspension containing soybean protein hydrolysate, which exhibited a moisture content of 1.17 ± 0.23% (db) and a_w of 0.43 ± 0.03.

3.2.2. Particle size

When produced, the SD-M $D_{4,3}$ was 8.90 ± 0.26 μm and $D_{0.5}$ 7.93 ± 0.19 μm with a span index of 1.42 ± 0.05. The SD-M powder showed a physical change (caking) during the first month of storage and the particle size could no longer be measured. The other studied microparticles samples (SCFO, DS26, DS40 and DS50) had a $D_{4,3}$ ranging between 18.57 ± 0.18 μm and 71.79 ± 0.41 μm, $D_{0.5}$ ranging between 17.65 ± 0.13 μm and 52.60 ± 0.07 μm and a span index between 1.71 ± 0.01 and 4.26 ± 0.10 (Table 3).

Karim *et al.* (2016) reported $D_{4,3}$ values for spray-dried microparticles loaded with fish oil ranging from 18.32 to 54.67 μm and concluded that the increase in feeding material viscosity increased microparticle sizes. The literature reports $D_{4,3}$ values of 24.2 to 38.7 μm for microencapsulated ginger oleoresin (Oriani *et al.* 2018) and higher sizes values for SLMs loaded with ascorbic acid (89.24 to 167.21 μm), which were attributed to the atomisation pressure used in the process (Matos *et al.* 2015).

All microparticle samples had higher $D_{4,3}$ values at 180 days of storage when compared to those of the newly produced samples (Table 3, lowercase letters), and this trend was particularly notable for double-shell microparticles stored at 24 ± 1 °C, mainly for the sample DS50 (Table 3, uppercase letters).

The particle size in the double-shell system was mostly affected by the percentage of core material and storage time rather than by the temperature or lipid wall material composition.

The span index decreased due to the increase in $D_{0.1}$ and $D_{0.5}$, suggesting agglomeration. In general, the particle size remained within the size range that is obtained by the equipment used. For food application, particle size should be smaller than 100 μm (Kaushik *et al.* 2015).

3.2.3. Colour

The lightness (L*) was affected by storage time and temperature. Samples stored at 6 ± 2 °C showed higher L* values (Table 4, uppercase letters). At both temperatures, L* value showed a tendency to decrease during storage, mainly for the SD-M (Table 4, lowercase letters). The SD-M had the highest ΔE, mainly when stored at 24 ± 1 °C, and the results suggested a tendency to red (+a*) and yellow (+b*). The increase in double-shell microparticle core concentration decreased L*, increased positive values for a* (redness) and b* (yellowness) and increased ΔE, mainly for those samples stored at 24 ± 1 °C, resulting in microparticle darkening.

The decrease in L* or the darkening of the samples could be a consequence of some factors as the moisture absorption and solubilisation of the grape juice, Maillard reaction products formed during the microparticles production and storage at 25 °C and anthocyanins degradation.

The studied microparticles showed a ΔE higher than 1.5, which means that a colour difference could be visually identified when comparing the stored samples with the newly produced ones (Obón *et al.* 2009). The SCFO and DS26 samples presented the highest L* values and the smallest ΔE, mainly when stored at

Table 4. Colour parameters of spray-dried microparticles loaded with fish oil (SD-M), spray-chilled microparticles loaded with fish oil (SCFO), double-shell microparticles loaded with 26 wt% of SD-M (DS26), double-shell microparticles loaded with 40 wt% of SD-M (DS40) and double-shell microparticles loaded with 50 wt% of SD-M (DS50) at zero, 90 and 180 days of storage at 6 ± 2 °C and 24 ± 1 °C (mean ± SD, where $n = 10$).

	Storage at 6 ± 2 °C				Storage at 24 ± 1 °C			
Days	L^*	a^*	b^*	ΔE^*	L^*	a^*	b^*	ΔE^*
SD-M Sample - spray-dried microparticles loaded with fish oil								
0	$89.11 \pm 0.01^{a,A}$	$2.45 \pm 0.02^{c,A}$	$7.18 \pm 0.01^{c,A}$		$89.11 \pm 0.01^{a,A}$	$2.45 \pm 0.02^{c,A}$	$7.18 \pm 0.01^{c,A}$	
90	$47.77 \pm 0.07^{b,A}$	$9.45 \pm 0.03^{b,B}$	$17.36 \pm 0.02^{b,B}$	$43.14 \pm 0.06^{b,B}$	$42.00 \pm 0.01^{b,B}$	$10.32 \pm 0.02^{b,A}$	$20.24 \pm 0.01^{b,A}$	$49.51 \pm 0.01^{b,A}$
180	$47.49 \pm 0.02^{c,A}$	$9.95 \pm 0.04^{a,B}$	$19.01 \pm 0.03^{a,B}$	$43.92 \pm 0.01^{a,B}$	$38.34 \pm 0.26^{c,B}$	$16.03 \pm 0.39^{a,A}$	$25.66 \pm 0.78^{a,A}$	$55.72 \pm 0.13^{a,A}$
SCFO Sample - spray-chilled microparticles loaded with fish oil								
0	$95.84 \pm 0.13^{c,A}$	$-0.47 \pm 0.01^{b,A}$	$4.27 \pm 0.01^{a,A}$		$95.84 \pm 0.13^{c,A}$	$-0.47 \pm 0.01^{c,A}$	$4.27 \pm 0.01^{c,A}$	
90	$97.80 \pm 0.08^{a,A}$	$-0.45 \pm 0.01^{c,B}$	$4.06 \pm 0.02^{c,B}$	$1.98 \pm 0.12^{a,A}$	$96.34 \pm 0.11^{a,B}$	$-1.11 \pm 0.02^{b,A}$	$5.85 \pm 0.02^{b,A}$	$1.78 \pm 0.05^{b,B}$
180	$97.57 \pm 0.05^{b,A}$	$-0.63 \pm 0.01^{a,B}$	$4.20 \pm 0.02^{b,B}$	$1.74 \pm 0.14^{b,B}$	$95.87 \pm 0.15^{b,B}$	$-1.24 \pm 0.01^{a,A}$	$6.59 \pm 0.05^{a,A}$	$2.45 \pm 0.05^{a,A}$
DS26 Sample - double-shell microparticles loaded with 26 wt% of SD-M								
0	$91.57 \pm 0.00^{a,A}$	$2.23 \pm 0.01^{b,A}$	$8.10 \pm 0.01^{c,A}$		$91.57 \pm 0.00^{a,A}$	$2.23 \pm 0.01^{b,A}$	$8.10 \pm 0.01^{c,A}$	
90	$90.46 \pm 0.01^{b,A}$	$2.11 \pm 0.02^{c,B}$	$9.35 \pm 0.00^{b,B}$	$1.67 \pm 0.00^{b,B}$	$89.35 \pm 0.01^{b,B}$	$2.28 \pm 0.01^{a,A}$	$13.52 \pm 0.01^{b,A}$	$5.85 \pm 0.01^{b,A}$
180	$89.16 \pm 0.01^{c,A}$	$2.29 \pm 0.01^{a,A}$	$10.73 \pm 0.00^{a,B}$	$3.56 \pm 0.01^{a,B}$	$88.88 \pm 0.01^{c,B}$	$2.17 \pm 0.02^{c,B}$	$15.37 \pm 0.01^{a,A}$	$7.75 \pm 0.01^{a,A}$
DS40 Sample - double-shell microparticles loaded with 40 wt% of SD-M								
0	$85.71 \pm 0.01^{b,A}$	$2.99 \pm 0.01^{c,A}$	$9.37 \pm 0.01^{c,A}$		$85.71 \pm 0.01^{a,A}$	$2.99 \pm 0.01^{c,A}$	$9.37 \pm 0.01^{c,A}$	
90	$85.73 \pm 0.00^{a,A}$	$3.16 \pm 0.02^{b,B}$	$11.36 \pm 0.00^{b,B}$	$2.00 \pm 0.01^{b,B}$	$80.36 \pm 0.05^{b,B}$	$4.56 \pm 0.02^{b,A}$	$19.28 \pm 0.01^{b,A}$	$11.38 \pm 0.02^{b,A}$
180	$84.60 \pm 0.01^{c,A}$	$3.48 \pm 0.01^{a,B}$	$12.97 \pm 0.01^{a,B}$	$3.81 \pm 0.01^{a,B}$	$77.82 \pm 0.01^{c,B}$	$4.60 \pm 0.20^{a,A}$	$21.19 \pm 0.01^{a,A}$	$14.31 \pm 0.01^{a,A}$
DS50 Sample - double-shell microparticles loaded with 50 wt% of SD-M								
0	$81.33 \pm 0.02^{a,A}$	$3.97 \pm 0.01^{c,A}$	$11.65 \pm 0.01^{c,A}$		$81.33 \pm 0.02^{a,A}$	$3.97 \pm 0.01^{c,A}$	$11.65 \pm 0.01^{c,A}$	
90	$78.76 \pm 0.01^{b,A}$	$4.28 \pm 0.02^{b,B}$	$13.97 \pm 0.00^{b,B}$	$3.47 \pm 0.01^{b,B}$	$74.51 \pm 0.01^{b,B}$	$5.69 \pm 0.02^{b,A}$	$21.77 \pm 0.00^{b,A}$	$12.32 \pm 0.00^{b,A}$
180	$78.64 \pm 0.01^{c,A}$	$4.51 \pm 0.01^{a,B}$	$15.68 \pm 0.00^{a,B}$	$4.88 \pm 0.01^{a,B}$	$72.95 \pm 0.01^{c,B}$	$7.62 \pm 0.02^{a,A}$	$27.32 \pm 0.01^{a,A}$	$18.15 \pm 0.01^{a,A}$

Different lowercase letters for the same sample at different storage times but the same temperature show significant differences among values ($p < 0.05$). Different uppercase letters for the same sample at the same storage time but different temperatures show significant differences among values ($p < 0.05$).

6 ± 2 °C. Depending on the food application, this characteristic can be important since the colour may influence product acceptability.

3.2.4. Morphology

At 180 days of storage, DS40 and DS50 samples presented some particle aggregation, mainly at 24 ± 1 °C (Figure 1), which can be mainly attributed to the higher moisture gain occurred during storage. The samples had rough surfaces and spherical shape. Lipid matrices with different types of triacylglycerols (TAGs) may result in solid lipid microparticles with crystals of different sizes and particles with rough surfaces (Matos *et al.* 2015).

3.2.5. EPA and DHA content

The reported losses of the studied PUFAs correspond to the sum of EPA and DHA losses. The comparison between the concentrations of these PUFAs in the SD-M with their initial concentrations in the feeding material indicates process losses of 0.8 wt%, that is in agreement with studies in which spray drying microencapsulation process preserved the fish oil PUFAs content and could be attributed to the short process time (Annamalai *et al.* 2015, Yeşilsu and Özyurt 2019, Ramos *et al.* 2021, Sultana *et al.* 2021).

The SCFO, DS26, DS40 and DS50 samples presented losses of PUFAs (EPA + DHA) due to the microencapsulation process of approximately 7.9 wt%, 8.7 wt%, 8.9 wt% and 2.8 wt%, respectively. Although the spray-chilling process uses low temperatures, the sample preparation and feeding step that occurred at 80 °C were responsible by the EPA and DHA losses.

At 180 days of storage at 6 ± 2 °C, the free fish oil presented PUFAs (EPA + DHA) losses of 7.6 wt% and when stored at 24 ± 1 °C the losses were of 87.3 wt%, suggesting that refrigerated storage was very important for preservation of PUFAs in the free fish oil.

The microparticles stored at 24 ± 1 °C had higher losses of EPA and DHA (Table 5, uppercase letters). Sultana *et al.* (2021) encapsulated Krill oil by spray drying using maltodextrin (DE 19) and emulsifiers and observed that after six months of storage at different temperatures the EPA and DHA losses were lower than 20% for the storage at 25 °C, and higher than 95% for the storage at 50 °C, since the temperature can favour the oxidation of PUFAs and form degradation compounds that can promote an autocatalytic reaction.

Storage time also significantly reduced the PUFAs levels, except for DS40, which had similar PUFAs losses at 90 and 180 days of storage at 24 ± 1 °C (Table 5, lowercase letters). At 180 days of storage, the DS26 sample stored at the lower temperature showed the best protection for EPA and DHA contents that could be attributed to more efficient entrapment of the core material (SD-M) within the lipid matrix. The lack of oxygen in a particle system will prevent the

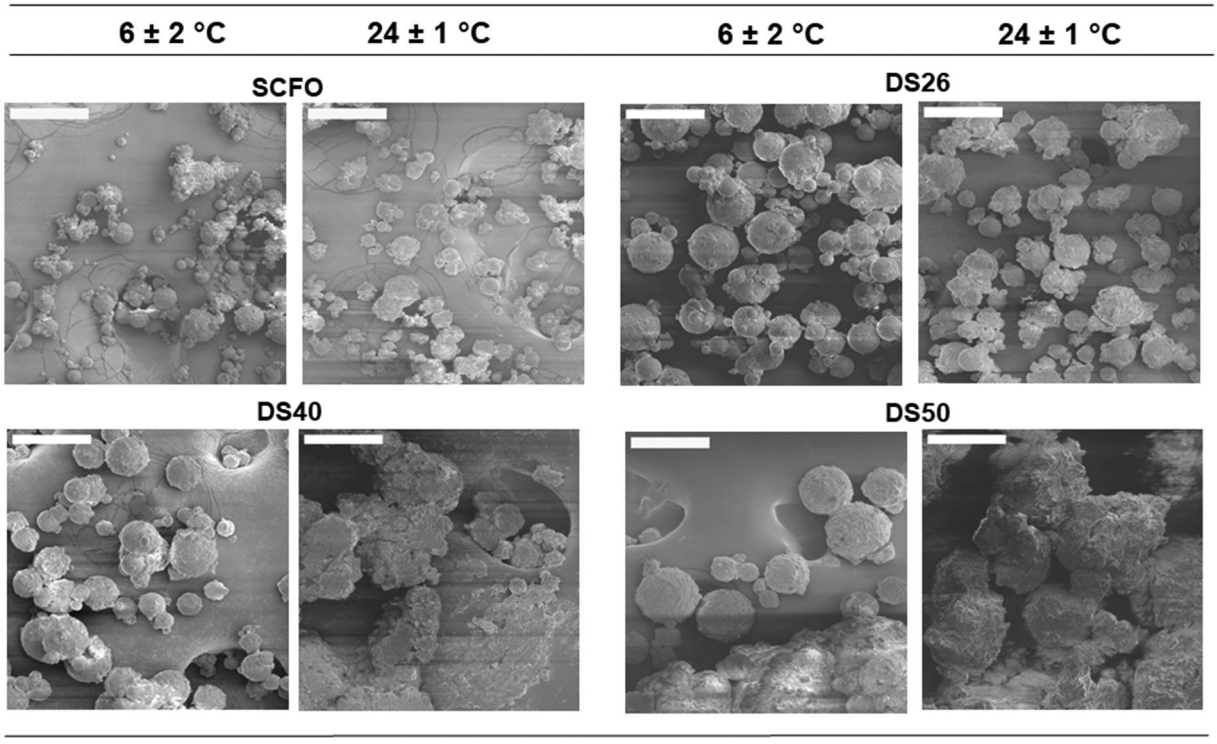

Figure 1. SEM micrographs showing the spray-chilled microparticles loaded with fish oil (SCFO), the double-shell microparticles loaded with 26 wt% of spray-dried microparticles loaded with fish oil (DS26), the double-shell microparticles loaded with 40 wt% of spray-dried microparticles loaded with fish oil (DS40) and the double-shell microparticles loaded with 50 wt% of spray-dried microparticles loaded with fish oil (DS50) at 180 days of storage at 6 ± 2 C and 24 ± 1 °C (200× magnification; the scale bars indicate 100 μm).

Table 5. EPA and DHA losses of spray-dried microparticles loaded with fish oil (SD-M), spray-chilled microparticles loaded with fish oil (SCFO), double-shell microparticles loaded with 26 wt% of SD-M (DS26), double-shell microparticles loaded with 40 wt% of SD-M (DS40) and double-shell microparticles loaded with 50 wt% of SD-M (DS50) comparing the PUFAs levels just after de microparticles production with the PUFAs levels observed at 90 and 180 days of storage at 6 ± 2 °C and 24 ± 1 °C (mean ± SD, where $n = 3$).

Days	Storage at 6 ± 2 °C EPA + DHA losses *(wt%)*	Storage at 24 ± 1 °C EPA + DHA losses *(wt%)*
	SD-M Sample - spray-dried microparticles loaded with fish oil	
90	$12.27 \pm 0.25^{b,B}$	$14.24 \pm 0.10^{b,A}$
180	$22.29 \pm 0.10^{a,B}$	$23.94 \pm 0.10^{a,A}$
	SCFO Sample - spray-chilled microparticles loaded with fish oil	
90	$1.20 \pm 0.21^{b,B}$	$13.24 \pm 0.21^{b,A}$
180	$10.35 \pm 1.04^{a,B}$	$25.63 \pm 0.96^{a,A}$
	DS26 Sample - double-shell microparticles loaded with 26 wt% of SD-M	
90	$8.03 \pm 0.10^{b,B}$	$11.31 \pm 0.10^{b,A}$
180	$8.76 \pm 0.10^{a,B}$	$15.33 \pm 0.10^{a,A}$
	DS40 Sample - double-shell microparticles loaded with 40 wt% of SD-M	
90	$14.18 \pm 0.10^{b,B}$	$23.69 \pm 0.63^{a,A}$
180	$16.32 \pm 0.01^{a,B}$	$24.63 \pm 0.24^{a,A}$
	DS50 Sample - double-shell microparticles loaded with 50 wt% of SD-M	
90	$16.28 \pm 0.51^{b,B}$	$26.92 \pm 0.47^{b,A}$
180	$26.62 \pm 0.27^{a,B}$	$28.82 \pm 0.51^{a,A}$

Different lowercase letters for the same sample at different storage times but the same temperature show significant differences among values ($p < 0.05$). Different uppercase letters for the same sample at the same storage time but different temperatures show significant differences among values ($p < 0.05$).

hydroperoxides formation in the fish oil and the subsequent decomposition in secondary oxidation products, therefore a wall matrix with oxygen diffusion barrier properties will be determinant to guarantee the desired protection (Linke *et al.* 2020b). Hinnenkamp *et al.* (2021) pointed out that although the emulsion characteristic and the EE usually impact the oxidative stability of the microencapsulated fish

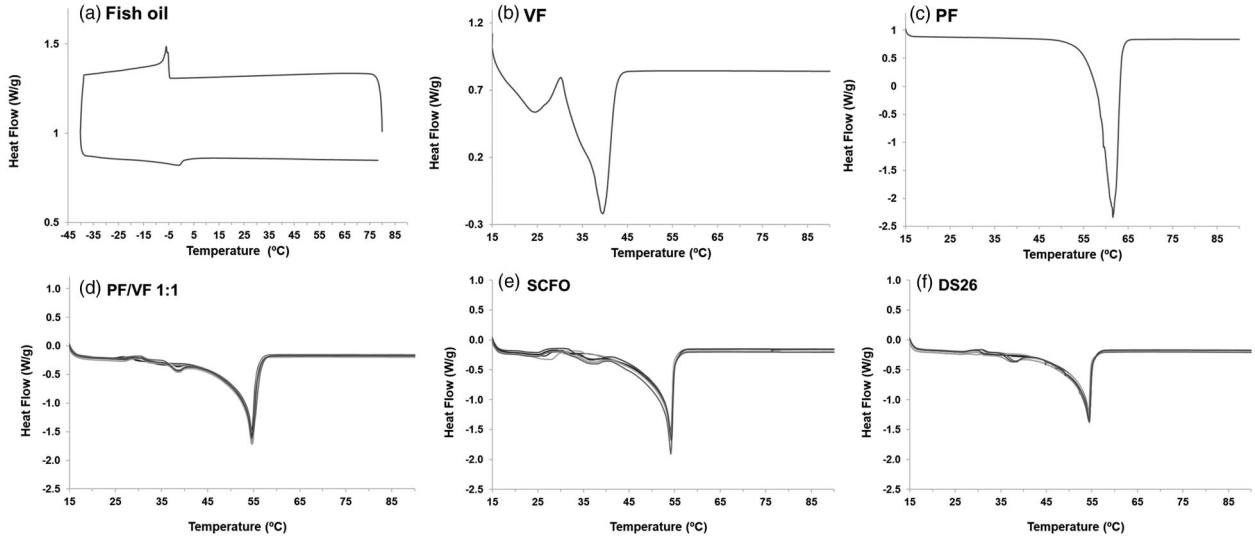

Figure 2. DSC thermograms of (a) fish oil, (b) vegetable fat (VF), (c) 100% hydrogenated palm oil (PF), (d) mixture of PF and VF 1:1 (control sample, empty microparticles), (e) spray-chilled microparticles loaded with fish oil (SCFO) and (f) double-shell microparticles (DS26) loaded with 26 wt% of spray-dried microparticles loaded with fish oil (SD-M), during 120 storage days at 25 ± 1 °C.

oil, at their study, the higher protein/peptides concentration in the wall material resulted in microparticles with lower peroxide and propanal levels since these wall material components could have scavenged radicals.

Microparticle characteristics have a great influence on the stability of encapsulated PUFAs, as well as the wall material composition, oil distribution within the particles, surface area, density, moisture content and water activity (Ghnimi *et al.* 2017). Double-shell microparticles had experienced increased moisture content and water activity values during storage, mainly those samples containing a high core load, which might have contributed to oil oxidation. In addition, the concentration of PUFAs was also reduced by the increase of moisture content. Therefore, high core material concentrations in the double-shell microparticles did not guarantee an extra protective effect to the fish oil. The overall oxidation is more dependent on the amount of encapsulated oil that is at high concentration than on the amount of non-encapsulated oil, although the superficial oil is exposed to the environmental oxygen and will oxidise faster than the encapsulated oil (Linke *et al.* 2020a).

Among the studied double-shell microparticles, the DS26 sample showed better maintenance of physical-chemical characteristics during storage with the lowest moisture gain and lowest losses of EPA and DHA. The DS26 sample along with the free fish oil, the individual lipid wall materials (PF and VF), the SCFO and a control empty spray-chilled sample (PF:VF, 1:1), underwent thermal property evaluation via DSC and crystalline structure identification via DRX (except the fish oil).

3.2.6. Thermal behaviour by differential scanning calorimetry (DSC)

The energy required for the phase change of melting and crystallisation of fish oil was 6.19 ± 0.07 J/g and 8.93 ± 0.07 J/g, respectively (Figure 2(a)). Tolstorebrov *et al.* (2014) observed that a significant share of fish oil remained liquid even at ultra-low temperatures (−100 °C), indicating the need for a packaging material with oxygen barrier properties and the use of vacuum. In our study, the minimum DSC operation temperature was −40 °C, and the obtained heat of fusion was very low, indicating that the fish oil liquid fraction was also significant.

The melting curve of vegetable fat (VF) presented a first melting peak temperature (T_{mp}) at 23.67 ± 0.23 °C and a ΔH_M of 41.04 ± 1.40 (J/g) and a second peak at 39.36 ± 0.45 °C and a ΔH_M of 80.58 ± 2.98 (J/g) (Figure 2(b)). This melting profile is very appropriated for fusion at corporal temperature. TAG chain length and the unsaturation level of their fatty acids influence the TAG melting point (Tolstorebrov *et al.* 2014); therefore, the first peak could be related to the fusion of mono-unsaturated TAGs, and the second peak could be related to the fusion of medium- and long-chain trisaturated TAGs with higher melting points. PF showed a sharp melting peak at 59.78 ± 0.20 °C and a ΔH_M of 163.65 ± 2.05 (J/g) (Figure 2(c)). The chain size of predominant TAGs found in PF was higher than that of

Table 6. Thermal properties of those microparticles samples with better maintenance of physical-chemical properties during the first storage study and that were selected for a second storage study during 120 days at 25 ± 1 °C (mean ± SD, where $n = 3$).

Storage days at 25 ± 1 °C	0	7	14	21	28	60	90	120
PF/VF (1:1) Control sample - empty spray-chilled microparticle sample								
Melting Temperature Peaks (Tmp °C)	$54.57 \pm 0.07^{a,b}$	54.63 ± 0.12^{a}	$54.56 \pm 0.18^{a,b}$	$54.45 \pm 0.19^{a,b}$	$54.53 \pm 0.02^{a,b}$	$54.56 \pm 0.07^{a,b}$	54.83 ± 0.13^{a}	54.06 ± 0.46^{b}
ΔH_M (J/g)	107.33 ± 0.49^{a}	113.30 ± 2.52^{a}	113.40 ± 1.71^{a}	112.13 ± 3.20^{a}	112.70 ± 3.81^{a}	113.83 ± 3.83^{a}	113.10 ± 2.40^{a}	113.80 ± 2.12^{a}
SCFO Sample - spray-chilled microparticle loaded with fish oil								
Melting Temperature Peaks (Tmp °C)	54.06 ± 0.01^{a}	53.95 ± 0.12^{a}	53.89 ± 0.08^{a}	54.03 ± 0.16^{a}	53.89 ± 0.11^{a}	54.06 ± 0.16^{a}	53.94 ± 0.07^{a}	54.10 ± 0.13^{a}
ΔH_M (J/g)	96.88 ± 0.53^{e}	97.52 ± 0.69^{e}	102.85 ± 1.20^{c}	$106.47 \pm 2.28^{b,c}$	$109.33 \pm 0.81^{a,b}$	$108.60 \pm 1.98^{a,b}$	111.00 ± 2.40^{a}	$108.50 \pm 0.57^{a,b}$
DS26 Sample - double-shell microparticles loaded with 26 wt% of SD-M								
Melting Temperature Peaks (Tmp °C)	54.43 ± 0.13^{a}	54.39 ± 0.06^{a}	54.39 ± 0.14^{a}	54.50 ± 0.00^{a}	54.51 ± 0.09^{a}	54.23 ± 0.08^{a}	54.31 ± 0.20^{a}	54.43 ± 0.11^{a}
ΔH_M (J/g)	76.18 ± 1.70^{c}	67.98 ± 1.82^{d}	$78.80 \pm 0.59^{b,c}$	$78.55 \pm 1.40^{b,c}$	$79.95 \pm 2.49^{a,c}$	$82.18 \pm 1.19^{a,b}$	84.69 ± 0.88^{a}	84.57 ± 2.63^{a}

PF: 100% hydrogenated palm oil; VF: vegetable fat obtained from fully hydrogenated and interesterified vegetable oils; SD-M: spray-dried microparticles loaded with fish oil.

TAGs found in VF and were observed to be TAGs with more than 48 carbons.

The newly produced control sample (PF:VF 1:1) had a T_{mp} at 54.57 ± 0.07 °C and a ΔH_M of 107.33 ± 0.49 (J/g) (Figure 2(d) and Table 6). This melting peak temperature was mostly influenced by TAGs with a number of carbon atoms of 50 (PPS) (21.1%), 52 (PSS) (19.7%) and 54 (SSS) (4.3%). Lopes *et al*. (2015) produced SLMs using hard fats with different TAG compositions and observed that melting peaks were influenced by TAG chain size. This result shows that the proposed wall material mixture resulted in a lipid matrix with excellent thermal resistance for food application.

When produced, the SCFO and DS26 samples also showed a T_{mp} of approximately 54 °C (Table 6), suggesting that the physical-chemical properties of lipid carriers were not affected by the core materials. These properties can be affected by a chemical interaction between the bioactive compound and the carrier in addition to the fact that the core material can act as an impurity, decreasing the peak temperature (Matos *et al*. 2015, Tulini *et al*. 2016). During storage, T_{mp} remained at 54 °C ($p < 0.05$), suggesting no fat crystal polymorphic transformation. Lipids predominantly contain three polymorphic forms, α (metastable), β′ (intermediately stability) and β (greatest stability and the highest melting point) (Ribeiro *et al*. 2015, Hondoh and Ueno 2016); therefore, changes in the melting temperature peak could indicate changes in polymorphic forms since all samples were stored under the same conditions. According to Ribeiro *et al*. (2015) the homogeneity of TAGs is directly related to the polymorphic transition rate; that is, fats with low variability of TAGs quickly turn into the β form, and fats with a random TAG distribution may indefinitely be in the β′ form, which suggests that the SLMs evaluated in our study could have the β′ crystal form. The melting temperature peaks observed in our study can guarantee microparticle physical stability at room temperature (Tulini *et al*. 2016, Carvalho *et al*. 2019).

The enthalpy of fusion is the energy necessary for melting fat crystals and homogeneous crystals, and crystalline structures require more energy to break down (Carvalho *et al*. 2019). Higher fusion enthalpy values were observed for the control sample, followed by those of the SCFO and DS26 samples. These results are in accordance with the sample composition, i.e. the addition of fish oil (SCFO sample) reduced this parameter due to the presence of polyunsaturated fat acids, and the DS26 sample was not 100% composed of lipids. The SCFO and DS26 samples showed some fluctuations in the ΔH_M during storage, which could be attributed to the need for a more homogeneous distribution of the core inside the lipid matrix or to the crystallinity that gradually increased.

According to Oriani *et al*. (2018) a crystal reorganisation in solid lipid microparticles during the storage could cause the core material expulsion and variations in enthalpy curve shape indicate changes in fat crystal polymorphic forms (Campos 2005). The studied microparticles showed no variations in enthalpy curves (Figure 2(d–f)), that is, the results suggest that there were no interactions between the core material (fish oil or SD-M) and the lipid wall material, no fat crystal changes due to the spray chilling process or the storage period and no fusion of the lipid matrix TAGs. Therefore, the direct microencapsulation of fish oil in the lipid matrix by spray chilling (SCFO) or the use of a double-shell system (DS26) resulted in microparticles with similar thermal resistance during all the period the DSC analysis were conducted (120 days) indicating that the studied microparticles samples are stable regarding the thermal parameters.

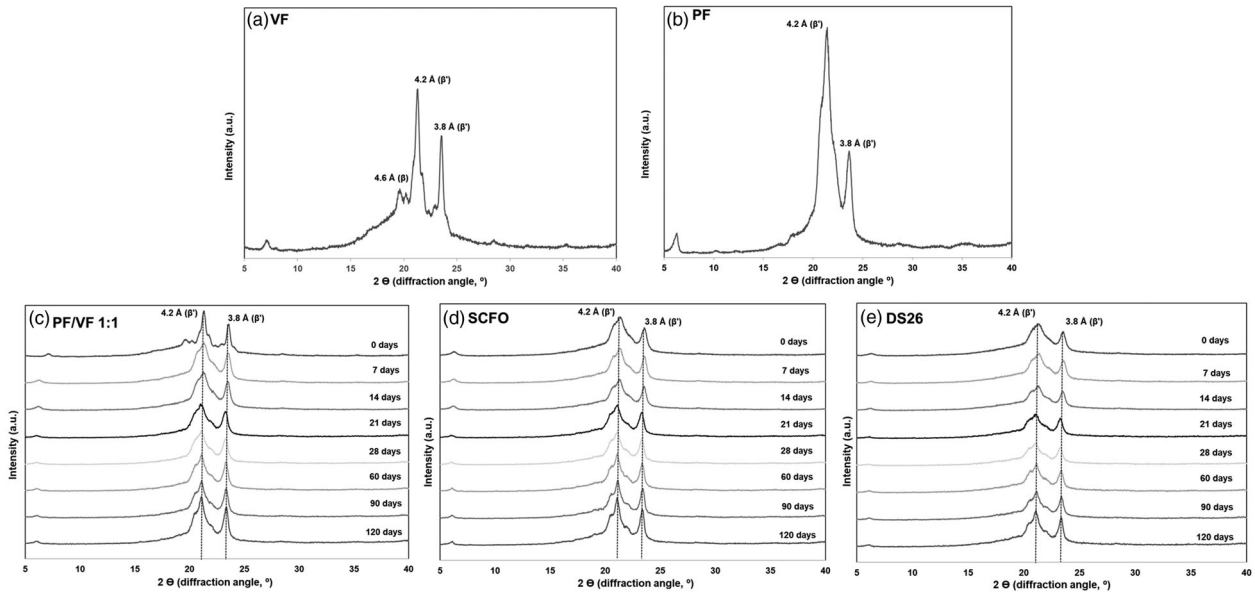

Figure 3. X-ray diffractograms of (a) vegetable fat (VF), (b) 100% hydrogenated palm oil (PF), (c) mixture of PF and VF 1:1 (control sample, empty microparticles), (d) spray-chilled microparticles loaded with fish oil (SCFO), and (e) double-shell microparticles (DS26) loaded with 26 wt% of spray-dried microparticles loaded with fish oil (SD-M), during 120 storage days at 25 ± 1 °C.

3.2.7. Crystalline structure

The crystalline structure of the lipids carriers (PF and VF), SCFO, DS26 and control sample were evaluated. The lipid carriers main abundant triacylglycerols (TAGs) were trisaturated species. The major TAG composition of the mixture of PF and VF (1:1) were LaLaLa, 6.9%; LaLaM, 7.9%; LaLaP, 6.5%; LaLaS, 10.4%; LaMS, 5.3%; LaSS, 7.7%; PPS, 21.1%, PSS, 19.7% and SSS, 4.3% (P, S, La and M correspond to the palmitic, stearic, lauric and myristic fatty acids, respectively).

During crystallisation, TAGs can pack in different polymorphic forms that will deflect X-rays at different angles. The α TAG polymorphic form has a hexagonal (H) subcell with a lattice spacing of 0.42 nm, the β′ form has an orthorhombic perpendicular ($O_{\perp}$) subcell with strong lattice spacing of 0.42–0.43 and 0.37–0.40 nm, and the β form, the most thermodynamic stable, has a triclinic parallel (T||) subcell with a strong lattice spacing of 0.46 nm (Ghotra *et al*. 2002, Campos 2005, Zheng *et al*. 2013, Ribeiro *et al*. 2015).

Lipid matrices with highly ordered lipid crystals limit the core material loading capacity and can expel it during storage. The numerous lattice defects shown in the β′ form crystal structure are favourable for good entrapment efficacy of the core material in SLMs (Jenning and Gohla 2001, Müller *et al*. 2002, Maschke *et al*. 2007, Okuro *et al*. 2013, Pelissari *et al*. 2016).

According to the results (Figure 3), the VF has most of the fatty crystals in the β′ polymorphic form, with a small proportion of β type crystals. The interesterification of lipid mixtures results in the formation of β′ type crystals attributed to the heterogeneous fatty acid radicals on the glycerol molecule (Jenab and Temelli 2013). In the PF the fatty crystals were exclusively in the β′ form.

The newly produced samples presented similar diffractograms between them, with two main peaks at the diffraction angles of 2θ of approximately 21° and 23° (with d spacings of 4.2 Å and 3.8 Å, respectively), typical for an orthorhombic subcell, indicating lipids in the β′ crystal polymorphic form (Figure 3). This result confirms that the blend of fats used did not affect the polymorphic stability and that the core material did not affect the crystal habit. According to DeMan and DeMan (2002), TAGs with 50 and 52 carbons are β′ formers. The lipid carrier mixture used in our study contained a TAG composition with 40.8% of the sum of C50 (PPS) and C52 (PSS). DeMan and DeMan (2002) noted that a TAG change into the β form increases the melting point. In our study, the β′ form did not present polymorphic alterations during storage, and the melting peak temperature did not change.

For food application, β′ fat crystals are more appropriate because they are small and soft, positive aspects for a good sensorial acceptance, mainly in fat-rich foods, such as bakery and confectionery products (Ribeiro *et al*. 2009, Tulini *et al*. 2017).

Therefore, according to the DSC and X-ray results the proposed lipid carrier mixture has an excellent compatibility since no liquefaction of the wall material and no change in the crystalline habit were observed during the storage period evaluated. The perfect

Table 7. Mean scores obtained by consumers ($n = 120$) in the acceptance test of chocolate dragees and cereal bars enriched with fish oil through the addition of the DS26 microparticles sample.

	Colour	Aroma	Taste	Texture	Overall Impression
Chocolate dragees	8.43 ± 0.56	8.10 ± 0.65	7.39 ± 0.93	7.94 ± 0.67	7.84 ± 0.66
Cereal bars	7.30 ± 1.18	7.38 ± 1.66	7.33 ± 1.35	7.65 ± 1.07	7.53 ± 0.98

DS26: double-shell microparticles loaded with 26 wt% of spray-dried microparticles loaded with fish oil (SD-M).

superposition of the DSC curves during storage, the maintaining of the melting peak temperature and the X-ray results can guarantee that the lipid matrix studied could be highly stable during storage at 25 °C for a long period of time. In conclusion, the studied double-shell microparticles have potential for both food application and to ensure the stability of the core material inside the lipid matrix during storage, provided that suitable packaging is used.

3.3. Food application and sensory acceptance test

The lipid carries used to produce the double-shell microparticles are ingredients found in many food products composition and according to their thermal stability it was expected that these microparticles would not deliver the fish oil in the oral phase digestion and the good results obtained in the sensory acceptance test of chocolate dragees and cereal bars added of the double-shell microparticles (DS26) confirmed that the fish oil release was not predominant in the oral phase digestion. Further studies are necessary to evaluate the release pattern during the storage period.

The SCFO sample had the characteristic fish oil flavour therefore this sample was not used for food application. The double-shell microparticles loaded with 26 wt% of SD-M were used to produce chocolate dragees and cereal bars. The products showed good sensory acceptance, with scores higher than 7.0 for all evaluated sensory attributes (Table 7). A score of 6.0 on a 9-point hedonic scale is considered a quality limit (Muñoz *et al.* 1992).

A consumer can accept or reject a food depending on various factors, such as the sensory characteristics of the product, their physiological status, previous information about the product and past experience, among others (Costell *et al.* 2010). The consumers who evaluated the chocolate dragees and cereal bars were previously informed about the fish oil addition to the products.

The consumers most liked the texture of the chocolate dragees (40%), followed by the taste (37%), aroma (26%) and colour (27%), and most disliked the taste (36%), followed by texture (12%), aroma (6%) and colour (3%). Among the consumers that did not like the taste of the chocolate dragees, 37.21% noticed the fish oil flavour, which corresponds to 13.3% of the total consumers. With respect to the cereal bar, consumers most liked the taste (48%), followed by the texture (33%), aroma (32%) and colour (9%), and the consumers most disliked the colour (26%), followed by the aroma (22%), taste (16%) and texture (15%). Among the consumers that did not like the taste of cereal bar, 53% noticed the fish oil flavour, which corresponds to 8% of the total consumers.

The microparticle thermal analysis showed that the peak area integration started at approximately 30 °C; therefore, the DS26 microparticles that were incorporated into the melted chocolate at 45 °C could have started releasing the core material earlier if compared to the cereal bar, where microparticles were incorporated at the lamination step, at a temperature of 36 °C. According to Okuro *et al.* (2013), bioactive compound release from lipid microparticles can be activated by the lipid matrix fusion in response to the increase in temperature therefore, some process adjustments should be made, especially in the production of chocolate dragees, to minimise the impact of temperature on the fish oil release, although the obtained results are very promising.

4. Conclusions

The losses of EPA and DHA occurred during the double-shell microparticles production were lower than 10 wt% and the spray-chilling step was the critical point, specifically the temperature used in the samples preparation and process feeding step (80 °C). Double-shell microparticles with 26 wt% of core material had moisture content, a_w and particle size appropriated to be used for food application and were more effective to protect EPA and DHA during storage at both temperatures. Double-shell microparticles (DS26) lipid matrix thermal stability could guarantee the good sensory acceptance of chocolate dragees and cereal bars enriched with EPA and DHA.

Acknowledgements

The authors are thankful to the Food Engineering Doctoral Program of UNICAMP (Brazil) and to the Brazilian National

Council for Scientific and Technological Development (CNPq) that provided scholarships to C.A. Carazzato and K.B.F. Paganotti.

Disclosure statement

The authors report no declarations of interest.

Funding

This work was supported by São Paulo Research Foundation (FAPESP) [Process 2015/12398–4].

ORCID

Ana Lúcia Fadini http://orcid.org/0000-0001-5618-0977
Izabela Dutra Alvim http://orcid.org/0000-0002-7882-5147
Camila Augusto Carazzato http://orcid.org/0000-0002-8295-6561
Katyri Bezerra de Freitas Paganotti http://orcid.org/0000-0002-1213-7296
Ana Maria Rauen de Oliveira Miguel http://orcid.org/0000-0003-4533-1885
Rodney Alexandre Ferreira Rodrigues http://orcid.org/0000-0001-5631-0970

References

Aghbashlo, M., *et al.*, 2013. Fish oil microencapsulation as influenced by spray dryer operational variables. *International journal of food science & technology*, 48 (8), 1707–1713.

Al-Ghannami, S.S., *et al.*, 2019. Randomized open-label trial of docosahexaenoic acid–enriched fish oil and fish meal on cognitive and behavioral functioning in Omani children. *Nutrition*, 57, 167–172.

Alvim, I.D., *et al.*, 2016. Comparison between the spray drying and spray chilling microparticles contain ascorbic acid in a baked product application. *LWT – Food science and technology*, 65, 689–694.

Annamalai, J., Dushyant C, K., and Gudipati, V., 2015. Oxidative stability of microencapsulated fish oil during refrigerated storage. *Journal of food processing and preservation*, 39 (6), 1944–1955.

AOCS 2017. American oil chemists society. Official method Ce 1a-13 (7th ed). Boulder, Urbana, IL: AOCS.

Bae, E.K., and Lee, S.J., 2008. Microencapsulation of avocado oil by spray drying using whey protein and maltodextrin. *Journal of microencapsulation*, 25 (8), 549–560.

Bakry, A.M., *et al.*, 2016. Microencapsulation of Oils: A Comprehensive Review of Benefits, Techniques, and Applications. *Comprehensive reviews in food science and food safety*, 15 (1), 143–182.

Binsi, P.K., *et al.*, 2017. Structural and oxidative stabilization of spray dried fish oil microencapsulates with gum arabic and sage polyphenols: Characterization and release kinetics. *Food chemistry*, 219, 158–168.

Bligh, E.G., and Dyer, W.J., 1959. A rapid method of total lipid extraction and purification. *Canadian journal of biochemistry and physiology*, 37 (8), 911–917.

Calder, P.C., 2014. Very long chain omega-3 (n-3) fatty acids and human health. *European journal of lipid science and technology*, 116 (10), 1280–1300.

Campos, R., 2005. Experimental methodology. *In*: A.G. Marangoni, ed. *Fat crystal networks*. Guelph: CRC Press, 267–348.

Carvalho, J.D.S., *et al.*, 2019. Characterization of ascorbic acid microencapsulated by the spray chilling technique using palm oil and fully hydrogenated palm oil. *LWT - Food science and technology*, 101, 306–314.

Chatterjee, S., and Judeh, Z.M.A., 2017. Impact of the type of emulsifier on the physicochemical characteristics of the prepared fish oil-loaded microcapsules. *Journal of microencapsulation*, 34 (4), 366–382.

Cho, Y.H., Shim, H.K., and Park, J., 2003. Encapsulation of fish oil by an enzymatic gelation process using transglutaminase cross-linked proteins. *Journal of food science*, 68 (9), 2717–2723.

Costell, E., Tárrega, A., and Bayarri, S., 2010. Food acceptance: The role of consumer perception and attitudes. *Chemosensory perception*, 3 (1), 42–50.

Croguennec, T., 2016. Lipid Oxidation. In: J. Romain, C. Thomas, S. Pierre, e B. Gérard, eds. *Handbook of food science and technology 1: Food alteration and food quality*. London: Wiley, 100–129.

DeMan, J. M., and DeMan, L., 2002. Polymorphis and texture of fats. In: N. Widlak, R. Hartel, e S. Narine, eds. *Crystallization and solidification properties of lipids*. Champaign, IL: AOCS Press, 225–235.

Di Giorgio, L., Salgado, P.R., and Mauri, A.N., 2019. Encapsulation of fish oil in soybean protein particles by emulsification and spray drying. *Food hydrocolloids*, 87, 891–901.

Encina, C., *et al.*, 2016. Conventional spray-drying and future trends for the microencapsulation of fish oil. *Trends in food science & technology*, 56, 46–60.

Fadini, A.L., *et al.*, 2018. Innovative strategy based on combined microencapsulation technologies for food application and the influence of wall material composition. *LWT - Food Science and Technology*, 91, 345–352.

Fadini, A.L., *et al.*, 2019. Optimization of the production of double-shell microparticles containing fish oil. *Food science and technology international*, 25 (5), 359–369.

Food Standards Agency 2002. *Mc Cance and Widdowson's. The composition of foods*. 6th ed. Cambridge: Royal Society of Chemistry.

Geranpour, M., Assadpour, E., and Jafari, S.M., 2020. Recent advances in the spray drying encapsulation of essential fatty acids and functional oils. *Trends in food science & technology*, 102, 71–90.

Ghnimi, S., Budilarto, E., and Kamal-Eldin, A., 2017. The new paradigm for lipid oxidation and insights to microencapsulation of omega-3 fatty acids. *Comprehensive reviews in food science and food safety*, 16 (6), 1206–1218.

Ghorbanzade, T., *et al.*, 2017. Nano-encapsulation of fish oil in nano-liposomes and its application in fortification of yogurt. *Food chemistry*, 216, 146–152.

Ghotra, B.S., Dyal, S.D., and Narine, S.S., 2002. Lipid shortenings: A review. *Food research international*, 35 (10), 1015–1048.

Haimeur, A., *et al.*, 2019. A comparative study on the effect of argan oil versus fish oil on risk factors for cardio-vascular disease in high-fat-fed rats. *Nutrition*, 57, 32–39.

Hartman, L., and Lago, R.C.A., 1973. Rapid preparation of fatty acid methyl esters from lipids. *Laboratory practice*, 22 (6), 475–476.

Hinnenkamp, C., Reineccius, G., and Ismail, B.P., 2021. Efficient encapsulation of fish oil: capitalization on the unique inherent characteristics of whey cream and hydrolyzed whey protein. *Journal of dairy science*, 104 (6), 6472–6486. article in press.

Hondoh, H., and Ueno, S., 2016. Polymorphism of edible fat crystals. *Progress in crystal growth and characterization of materials*, 62 (2), 398–399.

Jenab, E., and Temelli, F., 2013. Characterization of enzymatically interesterified canola oil and fully-hydrogenated canola oil blends under supercritical CO2. *JAOCS. Journal of the american oil chemists' society*, 90 (11), 1645–1652.

Jenning, V., and Gohla, S.H., 2001. Encapsulation of retinoids in solid lipid nanoparticles (SLN®). *Journal of microencapsulation*, 18 (2), 149–158.

Karim, F.T., *et al.*, 2016. Microencapsulation of fish oil using hydroxypropyl methylcellulose as a carrier material by spray drying. *Journal of food processing and preservation*, 40 (2), 140–153.

Kaushik, P., *et al.*, 2015. Microencapsulation of omega-3 fatty acids: A review of microencapsulation and characterization methods. *Journal of functional foods*, 19, 868–881.

Labuza, T.P., Kaanane, A., and Chen, J.Y., 2006. Effect of temperature on the moisture sorption isotherms and water activity shift of two dehydrated foods. *Journal of food science*, 50 (2), 385–392.

Lacerda, E.C.Q., *et al.*, 2016. Starch, inulin and maltodextrin as encapsulating agents affect the quality and stability of jussara pulp microparticles. *Carbohydrate polymers*, 151, 500–510.

Lavanya, M.N., *et al.*, 2020. Influence of spray-drying conditions on microencapsulation of fish oil and chia oil. *Drying technology*, 38 (3), 279–292.

Linke, A., Hinrichs, J., and Kohlus, R., 2020a. Impact of the powder particle size on the oxidative stability of microencapsulated oil. *Powder technology*, 364, 115–122.

Linke, A., Linke, T., and Kohlus, R., 2020b. Contribution of the internal and external oxygen to the oxidation of microencapsulated fish oil. *European journal of lipid science and technology*, 122 (8), 1900381, 1–10.

Linke, A., Weiss, J., and Kohlus, R., 2020c. Oxidation rate of the non-encapsulated- and encapsulated oil and their contribution to the overall oxidation of microencapsulated fish oil particles. *Food research international*, 127, 108705–9.

Lopes, J.D., *et al.*, 2015. Solid lipid microparticles of hardfats produced by spray cooling as promising crystallization modifiers in lipid systems. *European journal of lipid science and technology*, 117 (11), 1733–1744.

Marangoni, A. G., 2005. Crystallography. In: A.G. Marangoni, ed. *Fat crystal networks*. New York: CRC Press, 1–21.

Maschke, A., *et al.*, 2007. Development of a spray congealing process for the preparation of insulin-loaded lipid microparticles and characterization thereof. *European Journal of Pharmaceutics and Biopharmaceutics*, 65 (2), 175–187.

Matos, F.E., Jr., *et al.*, 2015. Development and characterization of solid lipid microparticles loaded with ascorbic acid and produced by spray congealing. *Food research international*, 67, 52–59.

Mohammed, N.K., *et al.*, 2020. Spray drying for the encapsulation of oils – A Review. *Molecules*, 25 (17), 3816–3873.

Müller, R.H., Radtke, M., and Wissing, S.A., 2002. Nanostructured lipid matrices for improved microencapsulation of drugs. *International journal of pharmaceutics*, 242 (1-2), 121–128.

Muñoz, A. M., Civille, G. V., and Carr, B. T., 1992. Comprehensive descreptive methode. In: A.M. Muñoz, G.V. Civille, and B.T. Carr, eds. *Sensory evaluation in quality control*. New York: Van Nostrand Reinhold., 52–107.

Murff, H.J., and Edwards, T.L., 2014. Endogenous Production of Long-Chain Polyunsaturated Fatty Acids and Metabolic Disease Risk. *Current cardiovascular risk reports*, 8 (12), 418.

Obón, J.M., *et al.*, 2009. Production of a red-purple food colorant from Opuntia stricta fruits by spray drying and its application in food model systems. *Journal of food engineering*, 90 (4), 471–479.

Okuro, P.K., *et al.*, 2013. Co- encapsulation of Lactobacillus acidophilus with inulin or polydextrose in solid lipid microparticles provides protection and improves stability. *Food research international*, 53 (1), 96–103.

Oriani, V.B., *et al.*, 2018. The influence of the storage temperature on the stability of lipid microparticles containing ginger oleoresin. *Food research international*, 109 (5), 472–480.

Pelissari, J.R., *et al.*, 2016. Production of solid lipid microparticles loaded with lycopene by spray chilling: Structural characteristics of particles and lycopene stability. *Food and bioproducts processing*, 98, 86–94.

Ramos, F.M., Júnior, V.S., and Prata, A.S., 2021. Impact of vacuum spray drying on encapsulation of fish oil: Oxidative stability and encapsulation efficiency. *Food research international*, 143, 110283.

Ribeiro, A.P.B., *et al.*, 2009. Instrumental methods for the evaluation of interesterified fats. *Food analytical methods*, 2 (4), 282–302.

Ribeiro, A.P.B., *et al.*, 2015. Crystallization modifiers in lipid systems. *Journal of food science and technology*, 52 (7), 3925–3946.

Roudaut, G., and Debeaufort, F., 2010. Moisture loss, gain and migration in foods and its impact on food quality. In: L.H. Skibsted, J. Risbo, e M.L. Andersen, eds. *Chemical deterioration and physical instability of food and beverages*. New York: CRC Press, 143–180.

Salvim, M.O., *et al.*, 2015. Production and structural characterization of solid lipid microparticles loaded with soybean protein hydrolysate. *Food research international*, 76, 3689–696.

Serfert, Y., Drusch, S., and Schwarz, K., 2010. Sensory odour profiling and lipid oxidation status of fish oil and microencapsulated fish oil. *Food chemistry*, 123 (4), 968–975.

Stone, H., and Sidel, J., 2004. *Sensory evaluation practices*. 3rd ed. San Diego, CA: Academic Press.

Sultana, A., *et al.*, 2021. Stability of eicosapentaenoic acid and docosahexaenoic acid in spray-dried powder of emulsified krill oil. *Future foods*, 3, 100009.

Tolstorebrov, I., Eikevik, T.M., and Bantle, M., 2014. A DSC determination of phase transitions and liquid fraction in fish oils and mixtures of triacylglycerides. *Food research international*, 58, 132–140.

Tulini, F.L., *et al.*, 2016. Development of solid lipid microparticles loaded with a proanthocyanidin-rich cinnamon extract (Cinnamomum zeylanicum): Potential for increasing antioxidant content in functional foods for diabetic population. *Food research international*, 85, 10–18.

Tulini, F.L., *et al.*, 2017. Evaluation of the release profile, stability and antioxidant activity of a proanthocyanidin-rich cinnamon (Cinnamomum zeylanicum) extract co-encapsulated with α-tocopherol by spray chilling. *Food research international*, 95, 117–124.

Yeşilsu, A.F., and Özyurt, G., 2019. Oxidative stability of microencapsulated fish oil with rosemary, thyme and laurel extracts: A kinetic assessment. *Journal of food engineering*, 240 (14), 171–182.

Zárate, R., *et al.*, 2017. Significance of long chain polyunsaturated fatty acids in human health. *Clinical and translational medicine*, 6 (1), 25.

Zheng, M., *et al.*, 2013. Formulation and characterization of nanostructured lipid carriers containing a mixed lipids core. *Colloids and surfaces A: Physicochemical and engineering aspects*, 430, 76–84.